MULTI-SCALE MODELING OF TWO-PHASE–TWO-COMPONENT PROCESSES IN HETEROGENEOUS POROUS MEDIA

JENNIFER NIESSNER[1] AND RAINER HELMIG[1]

[1]IWS, Department of Hydromechanics and Modeling of Hydrosystems, Universität Stuttgart, Germany

Abstract

Flow and transport phenomena in porous media are the governing processes in many natural and industrial systems. Not only do these flow and transport phenomena occur on different space and time scales, but it is also the porous medium itself which is heterogeneous where the heterogeneities are present on all spatial scales.

We consider a large domain with randomly distributed heterogeneities where complex two-phase–two-component processes are relevant only in a small (local) subdomain. This subdomain needs fine resolution as the complex processes are governed by small-scale effects. For a comprehensive fine-scale model taking into account two-phase–two-component processes as well as heterogeneities in the whole (global) model domain, data collection is expensive and computational time is high. Therefore, we developed a multi-scale concept where on the one hand, the global flow field influences the local two-phase–two-component processes on the fine-scale. On the other hand, a coarse-scale saturation equation is solved where the effects of the fine-scale two-phase–two-component processes in the subdomain are captured by source / sink terms and the effects of fine-scale heterogeneities by a macrodispersion term.

The overall algorithm as well as results will be discussed for simplified applications

1. INTRODUCTION

Flow and transport processes in porous media govern a variety of applications ranging from environmental engineering over technical applications to biosciences. In this work, we consider one of the classical applications in the field of environmental engineering where flow and transport of contaminants in the subsurface is considered, see e.g. (15), (6), (5). Figure 1 shows on the left hand side a schematic cut-out of the hydrosystem subsurface where the unsaturated zone above the ground-water table is contaminated by an LNAPL (light non-aqueous phase liquid) which is immiscible with water and of a density smaller than that of water. It can be seen, that

(a) the soil structure is heterogeneous. The distribution of small-scale heterogeneities has a high impact on all flow and transport processes.
(b) processes of different complexity occur in different parts of the soil which are characterized by a different number of phases p and a different number of components c. Around the LNAPL contamination, mass transfer processes play an important role, while further away from the plume, the mass transfer is negligibly small.

In this work, we study the simplified setup shown in Figure 1 on the right hand side where on the one hand, small-scale heterogeneities occur in the whole domain. On the

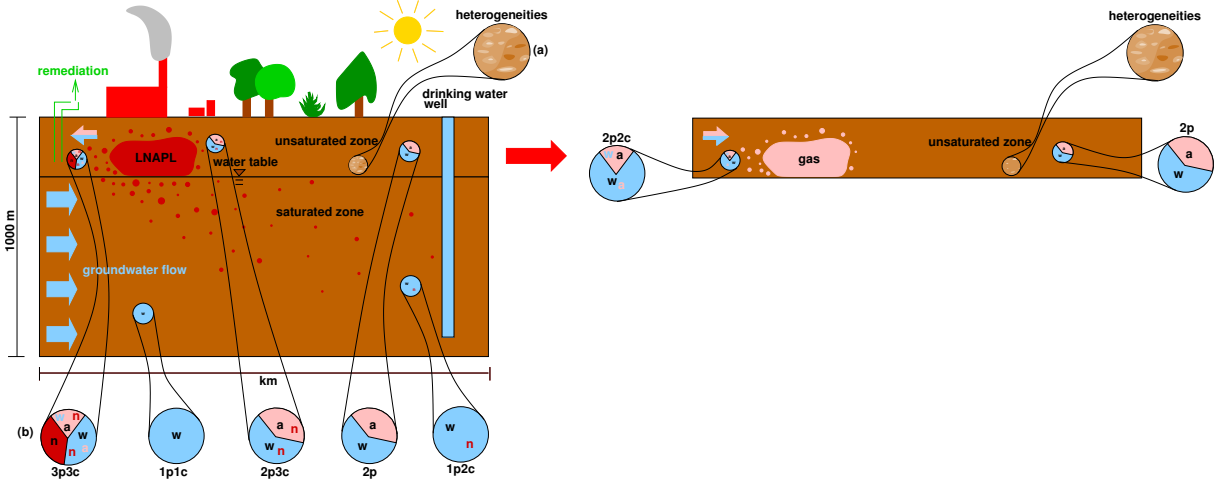

FIGURE 1. Processes in the hydrosystem subsurface (left hand side) and simplified system considered in this work (right hand side).

other hand, complex 2p2c processes occur in a small part of the model domain, around a zone where a high amount of gas is present. Further away from this zone, mass transfer processes become negligibly small and a 2p model is adequate. Detailed investigations on this subject can be found in (17).

To accurately capture the influence of both heterogeneities and mass-transfer processes, a fine-scale model is necessary, while for the physically simpler two-phase processes a coarser resolution already gives reasonable results.

To handle processes in heterogeneous systems occuring on different scales, different strategies can be persued. One of theses strategies is multi-scale modeling ((19), (18), (4), (16)), another one is upscaling (see e.g. (13) or (10)).

The aim of this work is to model the system shown in Figure 1 on the right hand side, where for the simpler 2p processes a mathematically motivated upscaling approach is applied allowing a coarse discretization while the complex 2p2c processes are modeled only locally and on a fine scale. Thus, the solution strategy consists of a combination of multi-scale modeling and upscaling where we use the semi-discrete upscaling concept of (12) and of (11) adapted to a discontinuous Galerkin finite element discretization.

As this work is a first step to model complex processes occuring on different scales, we reduce the complexity and neglect incompressibility of fluid phases and solid matrix, capillary pressure, gravity, as well as external sinks and sources.

In Section 2, we introduce the underlying mathematical model on the fine scale, while in Section 3, the numerical discretization is shortly introduced and reasons for the choice of the numerical scheme are given. Next, in Section 4, the combined upscaling–multi-scale solution strategy adequate for the modeling of systems like the one shown in Figure 1 on the right hand side is developed. After showing numerical results for this setup in Section 5, we sum up and give an outlook on future work in Section 6.

2. MATHEMATICAL MODEL ON THE FINE SCALE

In this section, we study the fine-scale equations necessary to describe two-phase flow (Section 2.1) and two-phase–two-component flow and transport (Section 2.2).

2.1. **Two-phase model.** We apply a fractional flow formulation of the governing equations taking into account the assumptions discussed in Section 1. The mass balance yields

$$\nabla \cdot \underline{v} = 0, \tag{1}$$

where $\underline{v} = \underline{v}_w + \underline{v}_n$ is the total velocity. The subscript w denotes the wetting phase, in our case the water phase and n denotes the non-wetting phase, i.e. the gas phase. The total velocity can be calculated as the sum of the extended Darcy laws for both phases as

$$\underline{v} = -\lambda \underline{\underline{K}} \nabla p. \tag{2}$$

The parameter λ is the total mobility defined as the sum of the phase mobilities λ_α, $\lambda = \lambda_w + \lambda_n = \frac{k_{rw}}{\mu_w} + \frac{k_{rn}}{\mu_n}$. Equation (2) serves as momentum balance equation.

Here, $\underline{\underline{K}}$ is the absolute permeability, $k_{r\alpha}$ denotes the relative permeability of phase α, μ_α is the respective viscosity, and p is the pressure of either phase. The equality of the phase pressures is due to the fact that we do not consider capillarity. The porosity of the medium does not occur in the equation as it is merely a rescaling factor of time. The relative permeability of each phase is usually a nonlinear function of the saturation S_α of that phase. In this work, we parameterize the functions $k_{r\alpha}(S_\alpha)$ using the approach of (3). The phase saturations sum up to 1, i.e. $S_w + S_n = 1$.

The *pressure equation* follows after inserting (2) in (1) and yields

$$\nabla \cdot \left[\lambda \underline{\underline{K}} \nabla p\right] = 0. \tag{3}$$

The second equation is that for the water saturation (the *saturation equation*):

$$\frac{\partial S_w}{\partial t} + \underline{v} \cdot \nabla f_w = 0, \tag{4}$$

with f_α as the fractional flow of the phase α calculated as $f_\alpha = \frac{\lambda_\alpha}{\lambda}$. This fine-scale saturation equation corresponds to the well-known Buckley-Leverett problem.

The pressure equation is of elliptic type, whereas the fine-scale saturation equation is hyperbolic.

2.2. **Two-phase–two-component model.** In a way analogous to the two-phase model given in Section 2.1, we can derive two equations for the total concentration C^κ of a component κ, i.e. in our case a component water (component 1) and a component air (component 2),

$$\frac{\partial C^\kappa}{\partial t} + \underline{v} \cdot \nabla \sum_\alpha (f_\alpha C_\alpha^\kappa) = 0 \qquad \kappa \in \{1, 2\} \tag{5}$$

The concentrations are calculated as $C_\alpha^\kappa = \rho_\alpha \cdot X_\alpha^\kappa$ and the total concentrations are defined as $C^\kappa = \rho_w S_w X_w^\kappa + \rho_n S_n X_n^\kappa$, with ρ_α as the density of phase α and X_α^κ as the mass fraction of component κ in phase α.

The concentration equations are hyperbolic and similar to the saturation equation except that the advective term is summed over the phases α. In practise, only one of the two concentration equations is solved. This concentration and the pressure are used in

flash calculations to reconstruct saturations. The usual flash calculations can either be a simple equilibrium ratio flash (so-called K^κ flash) which was first described by (20), or a more sophisticated approach where equality of the phase fugacities is assumed which can be solved either by iterative successive substitution or by a Newton–Raphson type procedure ((14)). In this work, we restrict ourselves to the simple approach of (20), i.e. a K^κ flash for a two-phase–two-component system.

3. NUMERICAL MODEL

The multi-scale–upscaling concept presented in this work and discussed in Section 4 represents a special challenge for numerical modeling. On the one hand, an accurate solution of the mathematical model requires a fine resolution, and thus, a fine grid. However, the purpose of this work implies to solve a coarse-scale model for saturation on a coarse grid. The consequence is usually high numerical diffusion and consequently, the solution is not very valuable any more. Therefore, to generate reliable results, it is on the one hand essential to use a numerical scheme which does not introduce too much numerical diffusion into the solution. On the other hand, it is planned to successively revoke the assumptions made in Section 1 later on. The decreasing ratio of advective over diffusive / dispersive processes might then change the mathematical character of the equations from hyperbolic to elliptic.

For these reasons, the discretization scheme applied to our multi-scale–upscaling framework are discontinuous Galerkin (DG) schemes, see (8), (7), (9), and (1) for the scheme used in this work. Being aware of the drawbacks of these schemes, we decided to apply them to all partial differential equations in the algorithm as the current implementation of the algorithm is a first step in the direction of the modeling of multi-scale–upscaling problems. For time discretization, we use Runge–Kutta schemes as they can be applied to explicit as well as to implicit schemes and as they easily allow use of higher order methods.

According to their mathematical character, we will solve the elliptic pressure equation using an implicit scheme. The hyperbolic-parabolic upscaled saturation equation as well as the concentration equations are solved time-explicitly. Further details can be taken from (17).

4. MULTI-SCALE–UPSCALING SOLUTION STRATEGY

The final aim of our multi-scale strategy is to model complex heterogeneous systems with locally occuring 2p2c processes while being computationally efficient. As these complex two-phase–two-component processes are dependent on small-scale effects, they are modeled on the local scale. In the rest of the domain, two-phase–two-component processes are of negligible impact. Therefore, a two-phase model is applied. This two-phase model is still dependent on local scale heterogeneities. However, it is possible to apply an upscaling approach to model only one of the two-phase equations on the local scale (the pressure equation), and to model an upscaled saturation equation on the macro scale. The upscaled saturation equation accounts for subgrid effects, i.e. local-scale heterogeneities, using a subgrid term.

A challenging task is the choice of the boundary conditions for the local two-phase–two-component problem. The problem is that they are dependent on the solution of the

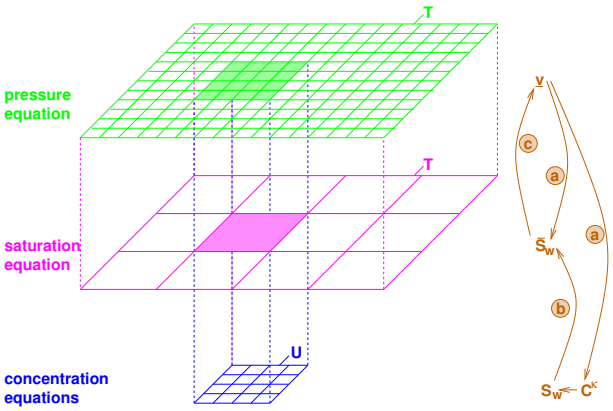

FIGURE 2. Overview of the solution strategy persued in this work.

global two-phase problem as the total concentrations are a function of saturation. That means, that these boundary conditions have to be updated each time step.

The issue of scales is directly related to the discretization scheme. The local-scale is associated with a fine resolution, i.e. a fine grid, whereas a macro-scale element contains a number of local-scale elements, i.e. we deal with a coarse grid on the macro scale. In this work, we will only use squared grids, although the equations presented are also valid for rectangular grids. Due to the fact, that saturation and concentration equations are solved time-explicitly, the *Courant-Friedrich-Lewy* (CFL) condition has to be fulfilled on the fine grid as well as on the coarse grid. This means, that a local time stepping has to be applied where the fine-grid concentration equations are solved using a local time step corresponding to the ratio of discretization lengths.

We will shortly discuss the upscaling of the saturation equation in Section 4.1 and then present our overall multiscale–upscaling algorithm in Section 4.2.

4.1. **Upscaling of the saturation equation.** To solve the saturation equation on a coarse grid, an upscaling approach has to be applied. In this work, the upscaling technique of volume averaging is chosen. The unknown parameters, water saturation S_w and total velocity $\underline{v}$ in our case, are averaged over the coarse-grid blocks A, i.e.

$$\underline{v} = \bar{\underline{v}} + \underline{v}', \quad S_w = \bar{S}_w + S_w' \qquad \text{with } \bar{\cdot} = \frac{1}{A}\int_A \cdot(\underline{x}, t)\, dA, \tag{6}$$

where the overbar denotes coarse-grid (block-averaged) quantities and the prime denotes fluctuating quantities.

The upscaled saturation equation for nonlinear relative permeabilities, as derived by (11), yields

$$\frac{\partial \bar{S}_w}{\partial t} + \frac{1}{A}\int_{d\Gamma} \bar{v}_j f_w(\bar{S}_w) n_j \, d\Gamma = \frac{\alpha}{A}\int_{d\Gamma} |v_i'(\underline{x},t)| \left(\frac{df_w(\bar{S}_w)}{d\bar{S}_w}\right)^2 \cdot \left(L_j \nabla_j \bar{S}_w - \frac{1}{2}(L_j \nabla_j \bar{S}_w)^2 \frac{d^2 f_w(\bar{S}_w)}{d\bar{S}_w^2}\right) n_i \, dl, \tag{7}$$

with L_j as the length of the coarse-grid streamline in the j direction. The coefficient $\alpha = (\sigma_K/2)^4$ accounts for the standard deviation σ_K of the log permeability field.

4.2. **Multi-scale solution algorithm.** Figure 2 gives an overview over the solution strategy. The pressure equation is solved in the whole domain on a fine grid, i.e. a small

scale, the local scale. The saturation equation is solved also in the whole domain, but in its upscaled form on a coarse grid, representing the macro scale. The concentration equations finally are solved only in a subdomain of the solution domain, where two-phase–two-component processes have a non-negligible influence. As they are highly dependent on local-scale processes, they are also solved on a fine grid, coinciding with the one that is used for the solution of the pressure equation.

From the solution of the pressure equation which gives the pressure field in the whole domain, we can calculate phase velocities $\underline{v}_\alpha$ and the total velocities $\underline{v}$. These velocities are needed for the solution of the upscaled saturation equation as well as for the solution of the concentration equations (a). After solving the pressure equation, the concentration equations are solved. The resulting quantities are the fine-grid total concentration. Using flash calculations, we can reconstruct saturations from the total concentrations which then enter (in averaged form) into the solution of the upscaled saturation equation (b). The new saturation distribution is then used to determine the pressure field of the next time step (c).

In the following, we call U the subdomain where 2p2c processes are relevant, whereas the total domain is denoted by T, see Figure 2. The basic assumption is that within the subdomain U, 2p2c processes are governing. That means, that the saturation distribution in U is determined by these processes. For the global saturation distribution (domain T), source / sink terms have to be introduced for all elements coinciding with the area of U in order to ensure a conservative solution of the saturation equation.

Let us now discuss our solution strategy to calculate one whole time step. As both saturation and concentration equation are solved explicitly in time, the CFL condition has to be fulfilled in both cases. For the saturation equation, the CFL condition has to be fulfilled on the coarse grid while for the concentration equations, it has to be fulfilled on the fine grid. Therefore, we have to apply a local time stepping and solve the concentration equations in several micro time steps such that the CFL condition is fulfilled on the fine grid using a micro time step and that it is fulfilled on the coarse grid using a macro time step. In the following, we will call the time step taken on the coarse grid "macro time step" or "time step", and the time step taken on the fine grid will be called "micro time step". At the beginning of a time step, we know the values of p, C^1, and $\bar{S}_w$ of the last time step.

(1) *Solve the modified fine-scale pressure equation in T:*

$$\nabla \cdot \left[\lambda(\bar{S}_w)\underline{\underline{K}} \cdot \nabla p\right] = 0, \qquad \underline{v}^{\text{discont.}} = -\lambda(\bar{S}_w)\underline{\underline{K}} \cdot \nabla p, \tag{8}$$

where we approximated the total mobility by the coarse-scale mobility $\lambda(\bar{S}_w)$.

(2) *Make the fine-scale velocity field in T continuous across element edges:* BDM_1^0 projection (see (2)): $\underline{v}^{\text{discont.}} \rightarrow \underline{v}^{\text{cont.}} := \underline{v} \rightarrow$ mass-conservativity.

(3) *Volume averaging for the total velocity $\underline{v}$ in T:* $\underline{v} = \bar{\underline{v}} + \underline{v}'$, $\qquad \bar{\underline{v}} = \frac{1}{h_E}\int_{\partial E} \underline{v}(\underline{x}, t)\, dl$ Linear interpolation of v_x and v_y between the edges.

(4) *Solve one fine-scale total concentration equation in U using micro time steps:*

$$\frac{\partial C^1}{\partial t} + \underline{v} \cdot \nabla \sum_\alpha (f_\alpha C_\alpha^1) = 0 \tag{9}$$

TABLE 1. Fluid and fluid–matrix parameters for the simulation example.

μ_w [kg/(ms)]	μ_n [kg/(ms)]	ρ_w [kg/m^3]	ρ_n [kg/m^3]	λ_{BC} [-]
1.0	1.0	1000.0	0.9	2.0

At ∂U: Dirichlet boundary conditions $C^1_D(\bar{S}^S_w)$ for the total concentration C^1:

$$C^1_D = \bar{S}^S_w \rho_w X^1_{w,D} + \bar{S}^S_n \rho_n X^1_{n,D}, \tag{10}$$

where the upper index S emphasizes that the saturation comes from the solution of the saturation equation calculated in step 8 of the last macro time step.

(5) *Calculate the fine-scale wetting-phase saturations in U from the concentration equation in U (flash calculations):* $S_w = S_w(C^1, p)$

(6) *Volume averaging for the saturation in U:* $S^C_w = \bar{S}^C_w + S'^C_w, \qquad \bar{S}^C_w = \frac{1}{A}\int_A S^C_w(\underline{x}, t)\, dA$
$\bar{S}^C_w$: saturations result from solution of concentration equation.

(7) *Ensuring mass conservativity of the coarse-scale saturation equation to be solved in 8:* $\bar{S}^C_w$ to be used for solution of upscaled saturation equation
$\rightarrow$ source / sink term to ensure local mass conservativity $q_w = \frac{\bar{S}^S_w - \bar{S}^C_w}{\partial t}$.

(8) *Solve the coarse-scale saturation equation in T:*

$$\frac{\partial \bar{S}_w}{\partial t} + \frac{1}{A}\int_{d\Gamma} \bar{v}_j f(\bar{S}_w) n_j d\Gamma = \frac{\alpha}{A}\int_{d\Gamma} |v'_i(\underline{x}, t)| \frac{d^2 f(\bar{S}_w)}{dS^2_w} \cdot \left(L_j \nabla_j \bar{S}_w - \frac{1}{2}(L_j \nabla_j \bar{S}_w)^2 \frac{d^2 f(\bar{S}_w)}{dS^2_w} \right) n_i \, dl + q_w \tag{11}$$

In the next section, we will apply the algorithm given by these eight steps to a simple test case. As our aim is to demonstrate the performance of this complex algorithm, the emphasis of the presented simulation was neither placed on the accurate choice of parameters nor on a high level of coarsening.

5. RESULTS

We consider a situation as given in Figure 1 on the right hand side where an initial higher non-wetting phase saturation is present in a certain subregion of a heterogeneous model domain and exposed to a flow from left to right. We use a geostatistically generated distribution of absolute permeability as shown in Figure 3. Absolute permeability is taken to be a scalar quantity here. The mean value is given as $\bar{K} = 10^{-10} m^2$, while the standard deviation of K is set to $\sigma_K = 1.5m$. The relative correlation length in x-direction is taken to be $l_x = 0.2$ (i.e. the correlation length is 20% of the length of the domain), the relative correlation length l_y in y-direction is $l_y = 0.01$, respectively. The fluid properties as well as the Brooks–Corey parameter λ_{BC} can be taken from Table 1. Flow is governed by the difference in the Dirichlet pressure boundaries as given in Figure 3, resulting in a mean total velocity of $1.5 \cdot 10^{-10} \frac{m}{s}$. The top and bottom boundary of domain T are impermeable (Neumann no-flow boundaries), while Dirichlet boundaries are assumed for the wetting-phase saturation, taking $S_w = 0.9$ at both left and right boundary. Initial conditions are given in a way that $S_w = 0.1$ in a small part V of the model domain T which lies inside the domain U. The initial and boundary conditions for C^1 are given in a way that applying a flash calculation the resulting wetting-phase saturation would be equal to $S_w = 0.9$ in $\{U \backslash V\}$ ($C^1 = 900 \frac{kg}{m^3}$), while within V, values for C^1 are given such that the resulting wetting-phase saturation $S_w = 0.1$, i.e., $C^1 = 100 \frac{kg}{m^3}$.

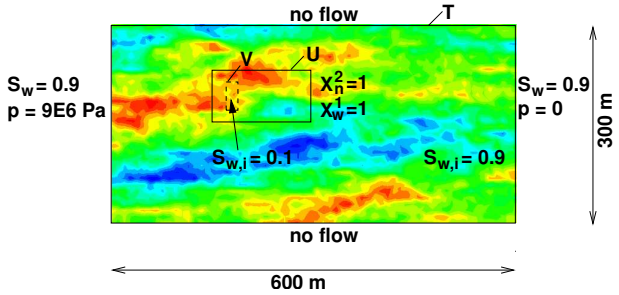

FIGURE 3. Setup for the test example.

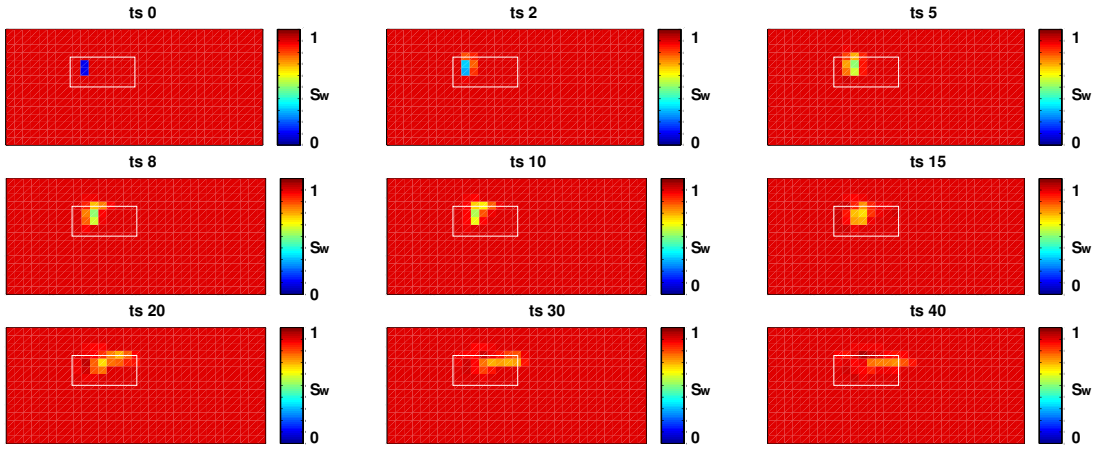

FIGURE 4. Simulation results after macro time steps 0, 2, 5, 8, 10, 15, 20, 30, and 40.

The discretization length is given by $\Delta x = 9.375$ m for the fine grid and $\Delta \bar{x} = 18.75$ m for the coarse grid. The results for different time steps can be taken from Figure 4.

6. SUMMARY AND OUTLOOK

We have so far presented the algorithm capable of combining processes occuring at different scales and in different overlapping domains in one model framework. The complex processes presented in this work are locally important mass transfer between a zone of high gas saturation and a surrounding water phase. The processes of the local and the global model as well as the processes on the fine and the coarse scale interact with each other. On the one hand, the global fine-scale flow field and the global coarse-scale saturation distribution influence the locally occuring fine-scale mass transfer processes, while on the other hand, the local fine-scale mass transfer determines the coarse-scale saturation distribution. Both fine-scale and coarse-scale processes are highly influenced by the heterogeneous structure of the model domain.

The solution strategy presented in this work is one first step to efficiently model and couple problems of different complexity occuring on different scales in one model framework. So far, the physics are still simplified. Further research has to be done to extend the model for a more complex physical and thermodynamic module to model real-life

systems. Especially the inclusion of capillarity and gravity as well as the compressibility of the gas phase have to be considered. Furthermore, non-isothermal processes might be included.

Further research has to be done to account for the fact that mass transfer is of highest importance at the interface between the gas plume and the surrounding groundwater, e.g. by a moving mesh following the plume.

As mentioned above, further improvement of the algorithm might be obtained by taking discretization schemes which are especially adapted for each process or equation type.

Finally, one might extend the model concept to account for other fine-scale effects than the local effect of misciblity, as for example local influence of compressibility.

Acknowledgements
We are grateful to the Landesgraduiertenföderung Baden-Württemberg and the SFB 404 "multifield problems in continuum mechanics" for funding this work.

References

1. P. Bastian, *Higher Order Discontinuous Galerkin Methods for Flow and Transport in Porous Media*, Challenges in Scientific Computing – CISC 2002 (E. Bänsch, ed.), LNCSE, no. 35, 2003.
2. F. Brezzi, J. Douglas, and L. D. Marini, *Recent results on mixed finite element methods for second order elliptic problems*, Optimization Software Publications, 1986.
3. A. N. Brooks and A. T. Corey, *Hydraulic properties of porous media*, Colorado State University, 1964.
4. Z. Chen and T. Y. Hou, *A mixed multiscale finite element method for elliptic problems with oscillating coefficients*, Mathematics of Computation **72** (2002), no. 242, 541–576.
5. H. Class and R. Helmig, *Numerical Simulation of Nonisothermal Multiphase Multicomponent Processes in Porous Media - 2. Applications for the Injection of Steam and Air*, Advances in Water Resources **25** (2002), 551–564.
6. H. Class, R. Helmig, and P. Bastian, *Numerical Simulation of Nonisothermal Multiphase Multicomponent Processes in Porous Media - 1. An Efficient Solution Technique*, Advances in Water Resources **25** (2002), 533–550.
7. B. Cockburn, S. Hou, and C.-W. Shu, *TVB Runge-Kutta local projection discontinuous Galerkin finite element method for conservation laws IV: The multidimensional case*, Journal of Mathematical Computation **54** (1990), 545–581.
8. B. Cockburn and C.-W. Shu, *TVB Runge-Kutta local projection discontinuous Galerkin finite element method for conservation laws II: General framework*, Journal of Mathematical Computation **52** (1989), no. 186, 411–435.
9. ———, *The Runge-Kutta Discontinuous Galerkin Method for Conservation laws V: Multidimensional Systems*, Journal of Computational Physics **141** (1998), 199–224.
10. L. J. Durlofsky, *Upscaling of Geocellular Models for Reservoir Flow Simulation: A Review of Recent Progress*, 7th International Forum on Reservoir Simulation, Bhl/Baden-Baden, Germany, June 23-27, 2003.
11. Y. Efendiev and L. J. Durlofsky, *Numerical modeling of subgrid heterogeneity in two phase flow simulations*, Water Resources Research **38** (2002), no. 8.

12. Y. Efendiev, L. J. Durlofsky, and S. H. Lee, *Modeling of subgrid effects in coarse-scale simulations of transport in heterogeneous porous media*, Water Resources Research **36** (2000), no. 8, 2031 – 2041.
13. R. E. Ewing, *Aspects of upscaling in simulation of flow in porous media*, Advances in Water Resources **20** (1997), no. 5-6, 349–358.
14. D. D. Fussel and J. L. Yanosik, *An iterative technique for compositional reservoir models*, SPE Journal, 1978.
15. R. Helmig, *Multiphase flow and transport processes in the subsurface*, Springer, 1997.
16. P. Jenny, S. H. Lee, and H. Tchelepi, *Multi-scale finite-volume method for elliptic problems in subsurface flow simulations*, J. Comp. Phys **187** (2003), 47–67.
17. J. Niessner, *Multi-scale modeling of two-phase–two-component processes in heterogeneous porous media*, Ph.D. thesis, Institute of Hydraulic Engineering, University of Stuttgart, 2006, in preparation.
18. E. Weinan and B. Engquist, *Multiscale modeling and computation* , Notices of the AMS **50** (2003), no. 9, 1062–1070.
19. E. Weinan, B. Engquist, and Z. Huang, *Heterogeneous multiscale method: A general methodology for multiscale modeling* , Physical Review **67** (2003).
20. L. C. Young and R. E. Stephenson, *A general compositional approach for reservoir simulation*, SPE Journal, 1983.